Mössbauer Characterization of the Iron−Sulfur Clusters in *Desulfovibrio vulgaris* Hydrogenase

Alice S. Pereira,[§,†] Pedro Tavares,[§,†] Isabel Moura,[†] José J. G. Moura,[†] and Boi Hanh Huynh*[,§]

Contribution from the Department of Physics, 1021 Rollins Research Building, Emory University, Atlanta, Georgia 30322, and Departamento de Química e Centro de Química Fina e Biotecnologia, Faculdade de Ciências e Tecnologia, Universidade Nova de Lisboa, 2825-114 Caparica, Portugal

Received August 25, 2000. Revised Manuscript Received December 29, 2000

Abstract: The periplasmic hydrogenase of *Desulfovibrio vulgaris* (Hildenbourough) is an all Fe-containing hydrogenase. It contains two ferredoxin type [4Fe-4S] clusters, termed the F clusters, and a catalytic H cluster. Recent X-ray crystallographic studies on two Fe hydrogenases revealed that the H cluster is composed of two sub-clusters, a [4Fe-4S] cluster ($[4Fe\text{-}4S]_H$) and a binuclear Fe cluster ($[2Fe]_H$), bridged by a cysteine sulfur. The aerobically purified *D. vulgaris* hydrogenase is stable in air. It is inactive and requires reductive activation. Upon reduction, the enzyme becomes sensitive to O_2, indicating that the reductive activation process is irreversible. Previous EPR investigations showed that upon reoxidation (under argon) the H cluster exhibits a rhombic EPR signal that is not seen in the as-purified enzyme, suggesting a conformational change in association with the reductive activation. For the purpose of gaining more information on the electronic properties of this unique H cluster and to understand further the reductive activation process, variable-temperature and variable-field Mössbauer spectroscopy has been used to characterize the Fe−S clusters in *D. vulgaris* hydrogenase poised at different redox states generated during a reductive titration, and in the CO-reacted enzyme. The data were successfully decomposed into spectral components corresponding to the F and H clusters, and characteristic parameters describing the electronic and magnetic properties of the F and H clusters were obtained. Consistent with the X-ray crystallographic results, the spectra of the H cluster can be understood as originating from an exchange coupled [4Fe-4S]−[2Fe] system. In particular, detailed analysis of the data reveals that the reductive activation begins with reduction of the $[4Fe\text{-}4S]_H$ cluster from the 2+ to the 1+ state, followed by transfer of the reducing equivalent from the $[4Fe\text{-}4S]_H$ subcluster to the binuclear $[2Fe]_H$ subcluster. The results also reveal that binding of exogenous CO to the H cluster affects significantly the exchange coupling between the $[4Fe\text{-}4S]_H$ and the $[2Fe]_H$ subclusters. Implication of such a CO binding effect is discussed.

Hydrogenases are a class of Fe−S proteins that catalyze the reversible reaction of $H_2 \leftrightarrow 2H^+ + 2e^-$, and many microorganisms use hydrogenase to metabolize H_2. They are a heterogeneous group of enzymes that differ in size, subunit composition, metal content, and cellular location, and the presence of multiple hydrogenases in a single organism has been reported. On the basis of their metal contents, however, two major groups of hydrogenases may be identified: the Fe hydrogenases, which contain only Fe,[1] and the Ni−Fe hydrogenases, which contain both Ni and Fe.[2] The periplasmic hydrogenase of *Desulfovibrio vulgaris* (Hilldenbourough) belongs to the Fe hydrogenase category.[3] It is an $\alpha\beta$ heterodimeric molecule with subunit molecular masses of approximately 46 and 10 kDa.[4,5] Metal content determinations showed varied Fe stoichiometry, probably due to the difficulties involved in protein determination and the possible presence of apoproteins or proteins lacking a full complement of metal. Values of 9−14 Fe/molecule[3] and 12−16 Fe/molecule[6,7] have been reported. Previous spectroscopic studies[3,7−9] and nucleotide-derived amino acid sequence analysis[4] suggested that eight of the iron atoms are organized into two ferredoxin-like $[4Fe\text{-}4S]^{+,2+}$ clusters, termed the F clusters, at the N-terminal region of the large subunit. The remaining Fe atoms form the catalytic center, termed the H cluster, which exhibits unusual electron paramagnetic resonance (EPR) spectra that are distinct from those of ferredoxin-type [4Fe-4S] clusters.[3,9,10] Recently, the X-ray crystallographic structure of the *D. desulfuricans* Fe hydrogenase, which has an

* Author for correspondence: Boi Hanh Huynh, Department of Physics, 1021 Rollins Research Building, Emory University, Atlanta, GA 30322. Telephone: (404) 727-4295. Fax: (404) 727-0876. E-mail: vhuynh@emory.edu.

§ Emory University.

† Universidade Nova de Lisboa.

(1) Adams, M. W. W. *Biochim. Biophys. Acta* **1990**, *1020*, 115−145.

(2) Przybyla, A. E.; Robbins, J.; Menon, N.; Peck, H. D., Jr. *FEMS Microbiol. Rev.* **1992**, *88*, 109−135.

(3) Huynh, B. H.; Czechowski, M. H.; Krüger, H. J.; DerVartanian, D. V.; Peck, H. D., Jr.; LeGall, J. *Proc. Natl. Acad. Sci. U.S.A.* **1984**, *81*, 3728−3732.

(4) Voordouw, G.; Brenner, S. *Eur. J. Biochem.* **1985**, *148*, 515−520.

(5) Prickril, B. C.; Czechowski, M. H.; Przybyla, A. E.; Peck, H. D., Jr.; LeGall, J. *J. Bacteriol.* **1986**, *167*, 722−725.

(6) Hagen, W. R.; Van Berkel-Arts, A.; Krüse-Wolters, K. M.; Voordouw, G.; Veeger, C. *FEBS Lett.* **1986**, *203*, 59−63.

(7) Pierik, A. J.; Hagen, W. R.; Redeker, J. S.; Wolbert, R. B. G.; Boersma, M.; Verhagen, M. F. J. M.; Grande, H. J.; Veeger, C.; Mutsaers, P. H. A.; Sands, R. H.; Dunham, W. R. *Eur. J. Biochem.* **1992**, *209*, 63−72.

(8) Grande, H. J.; Dunham, W. R.; Averill, B.; Van Dijk, C.; Sands, R. H. *Eur. J. Biochem.* **1983**, *136*, 201−207.

(9) Patil, D. S.; Moura, J. J. G.; He, S. H.; Teixeira, M.; Prickril, B. C.; DerVartanian, D. V.; Peck, H. D., Jr.; LeGall, J.; Huynh, B. H. *J. Biol. Chem.* **1988**, *263*, 18732−18738.

(10) Hagen, W. R.; Van Berkel-Arts, A.; Krüse-Wolters, K. M.; Dunham, W. R.; Veeger, C. *FEBS Lett.* **1986**, *201*, 158−162.

10.1021/ja003176+ CCC: $20.00
Published on Web 03/02/2001

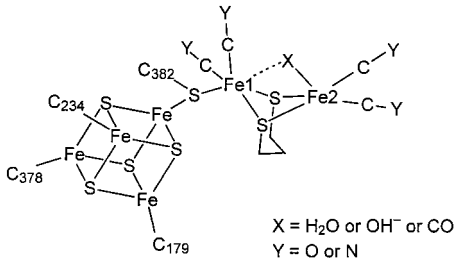

Figure 1. Schematic representation of H cluster based on the X-ray crystallographic structure of *D. desulfuricans* hydrogenase.[11,14]

identical amino acid sequence with the periplasmic *D. vulgaris* hydrogenase, has been solved and reveals a most unusual structure for the H cluster.[11] It is formed with two sub-clusters, a ferredoxin-type [4Fe-4S] cluster ($[4Fe\text{-}4S]_H$) and a binuclear Fe cluster ($[2Fe]_H$), bridged by a cysteine sulfur (C382) (Figure 1). In addition to the cysteine S ligand to Fe1, each Fe atom of the binuclear cluster is coordinated to one CO, one CN^-, an asymmetrically bridging mono-atomic oxygen species, and two bridging thiolates of a 1,3-propanedithiol group. The assignments for the diatomic ligands are based on evidence provided by infrared spectroscopic studies.[12] A similar structure has also been reported for the H cluster of the Fe hydrogenase I from *Clostridium pasteurianum*.[13] For *C. pasteurianum* hydrogenase I, a diatomic molecule was found to bridge the two Fe atoms of the binuclear $[2Fe]_H$ subcluster in place of the bridging mono-atomic ligand in *D. desulfuricans* hydrogenase. In a later review article, however, Nicolet et al.[14] commented that the electron density initially interpreted as an asymmetrically bridged water molecule could also be interpreted as a partially disordered diatomic ligand.

Fe hydrogenases are generally found in strict anaerobes. Most of the Fe hydrogenases exhibit extreme sensitivity toward molecular oxygen and have to be purified under anaerobic conditions. The *D. vulgaris* hydrogenase, on the other hand, can be purified aerobically, and the purified enzyme is stable in air. The aerobically purified enzyme, however, is inactive and requires a reductive activation. Upon reduction, the enzyme becomes air-sensitive, indicating that the reductive process is irreversible. EPR spectroscopy has been used to investigate this reductive process,[7,9] and four EPR signals were detected during the reduction.[9] In the as-purified enzyme, an "isotropic" $g = 2.02$ signal indicative of a $[3Fe\text{-}4S]^+$ cluster is observed. Depending on the preparation, the intensity of this signal varies between 0.02 and 0.2 spin/molecule. This signal is therefore attributed to a $[3Fe\text{-}4S]^+$ impurity resulting from oxidative damage of the [4Fe-4S] clusters. At a potential of about 0 mV (vs normal hydrogen electrode), a rhombic EPR signal with g values at 2.06, 1.96, and 1.89 (the rhombic 2.06 signal) begins to appear and reaches a maximum intensity of ~0.7 spin/molecule at about −110 mV. Upon further reduction, this rhombic 2.06 signal disappears and is replaced by another rhombic signal having g values at 2.10, 2.04 and 2.00 (rhombic 2.10 signal). The intensity of this rhombic 2.10 signal maximizes at about −300 mV accounting for approximately 0.4 spin/molecule. Below −320 mV, the signal abruptly disappears. A fourth EPR signal representing two dipolar-coupled $[4Fe\text{-}4S]^+$ clusters[8] appears at potentials below −250 mV and reaches its maximum intensity of 2 spins/molecule at −350 mV.[9] Reoxidation of the enzyme under anaerobic conditions yields only the rhombic 2.10 signal.[7]

The rhombic 2.10 signal has been observed for all Fe hydrogenases that have been investigated by EPR spectroscopy[1] and has been assigned to the H cluster. Since this signal is observed in the reoxidized *D. vulgaris* hydrogenase as well as in the as-purified forms of other Fe hydrogenases that were purified anaerobically, the rhombic 2.10 signal has been assigned to the "oxidized" form of the active H cluster (H_{OX}). Although the g values of the rhombic 2.06 signal are similar to those of $[4Fe\text{-}4S]^+$ clusters, it appears at a potential that is almost 300 mV above the potential at which a ferredoxin-type [4Fe-4S] cluster would be reduced. Furthermore, the signal can be detected without any observable broadening at a temperature (e.g., 40 K) at which the signal of a ferredoxin-type $[4Fe\text{-}4S]^+$ cluster would be broadened beyond detection. On the basis of these unusual properties, the rhombic 2.06 signal was also assigned to the H cluster.[9] If the conversion of the rhombic 2.06 to the rhombic 2.10 signal were to represent a reduction at the H cluster, it would have to be a two-electron reduction step since both signals are arising from a spin $S = {}^1/_2$ state. Such a step was considered to be unlikely, and instead, the conversion of rhombic 2.06 to 2.10 signal was suggested to reflect a conformational change at the H cluster associated with the irreversible reductive activation.[9]

Similar to other Fe hydrogenases, the *D. vulgaris* hydrogenase is highly sensitive to inhibition by CO. Reacting the fully reduced enzyme with CO results in the appearance of an axial EPR signal with resonances at $g_{\|} = 2.06$ and $g_{\perp} = 2.01$, termed the axial 2.06 signal.[15−17] This signal is photosensitive. At temperatures below 10 K, illumination of the CO-reacted enzyme with white light quantitatively converted the axial 2.06 signal to the rhombic 2.10 signal. Warming the sample to 150 K reversed this photoinduced process and restored the axial 2.06 signal.[17] These observations indicate that the axial 2.06 signal also arises from the H cluster and represents an "oxidized" H cluster coordinated to a photodissociable CO ligand. Reacting the anaerobically purified *C. pasteurianum* hydrogenases I and II with CO yields similar photosensitive axial 2.06-type signals, which also convert to the rhombic 2.10 signals upon illumination at 8 K.[1,18] Illumination of the *C. pasteurianum* hydrogenases at higher temperature (e.g., 30 K), however, generated a different photoproduct displaying an EPR signal with $g = 2.26$, 2.12, and 1.89.[1,18]

For the purpose of gaining more information on the electronic properties of this unique H cluster and to understand further the reductive activation process, we have used Mössbauer spectroscopy to characterize in detail the Fe−S clusters in *D. vulgaris* hydrogenase at different redox states generated during a reductive titration of the aerobically purified enzyme and in the CO-reacted enzyme. The results not only provide information on the electronic properties of the H cluster, but also indicate that conversion of the rhombic 2.06 to 2.10 signal is associated with the transfer of an electron from the $[4Fe\text{-}4S]_H$ subcluster to the binuclear $[2Fe]_H$ subcluster. The results also reveal that

(11) Nicolet, Y.; Piras, C.; Legrand, P.; Hatchikian, C. E.; Fontecilla-Camps, J. C. *Structure (London)* **1999**, *7*, 13−23.
(12) Pierik, A. J.; Hulstein, M.; Hagen, W. R.; Albracht, S. P. J. *Eur. J. Biochem.* **1998**, *258*, 572−578.
(13) Peters, J. W.; Lanzilotta, W. N.; Lemon, B. J.; Seefeldt, L. C. *Science (Washington, D. C.)* **1999**, *282*, 1853−1858.
(14) Nicolet, Y.; Lemon, B. J.; Fontecilla-Camps, J. C.; Peters, J. W. *Trends Biochem. Sci.* **2000**, *25*, 138−143.
(15) Patil, D. S.; Czechowski, M. H.; Huynh, B. H.; LeGall, J.; Peck, H. D., Jr.; DerVartanian, D. V. *Biochem. Biophys. Res. Commun.* **1986**, *137*, 1086−1093.
(16) Patil, D. S.; He, S. H.; DerVartanian, D. V.; Le Gall, J.; Huynh, B. H.; Peck, H. D., Jr. *FEBS Lett.* **1988**, *228*, 85−88.
(17) Patil, D. S.; Huynh, B. H.; He, S. H.; Peck, H. D., Jr.; DerVartanian, D. V.; LeGall, J. *J. Am. Chem. Soc.* **1988**, *110*, 8533−8534.
(18) Kowal, A. T.; Adams, M. W. W.; Johnson, M. K. *J. Biol. Chem.* **1989**, *264*, 4342−4348.

Table 1. Mössbauer Quantification of the Fe−S Clusters in the Samples of *D. vulgaris* Hydrogenase[a]

	F cluster		H cluster				
sample	$[4Fe\text{-}4S]^{2+}$	$[4Fe\text{-}4S]^{+}$	H_{OX+1}	$H_{OX-2.06}$	$H_{OX-2.10}$	H_{red}	H_{OX}-CO
as-purified	2	0	1.0	0	0	0	0
−110 mV	2	0	0.37	0.63	0	0	0
−310 mV	1.8	0.2	0	0	0.5	0.5	0
−350 mV	0	2	0	0	0	1.0	0
CO-reacted	1.1	0.9	0	0	0	0	1.0

[a] The stoichiometry for each Fe−S species is calculated from the percent Fe absorption obtained for that particular species. Our analysis indicates that the two F clusters contribute 57% and the H cluster contributes 43% to the total Fe absorption (not counting the [3Fe-4S] impurity), consistent with the Fe contents associated with these two types of clusters in an enzyme molecule (8 Fe atoms for the two F clusters and 6 Fe atoms for the H cluster).

binding of an exogenous CO affects the exchange coupling between the two subclusters. Implication of such a CO binding in correlation with recent crystallographic findings of CO binding to Fe2[19,20] is discussed.

Methods

Sample Preparation. The ^{57}Fe-labeled *D. vulgaris* hydrogenase was purified from cells grown in ^{57}Fe-enriched medium as described in the literature.[3,9] Reductive activation of the enzyme was performed according to procedures used in the previous EPR reductive titration studies.[9] Mössbauer samples (200 μM protein in 200 mM Tris-HCl buffer at pH 7.0) were prepared at potentials of −110, −310, and −350 mV to maximize the accumulations of the rhombic 2.06, rhombic 2.10, and fully reduced state, respectively. Parallel EPR samples were prepared to ascertain the states of the Mössbauer samples. Results of the EPR samples have been published previously[9] and indicated maximum accumulations of the intended species (0.7 and 0.4 equiv for the rhombic 2.06 and 2.10 species, respectively). The CO-reacted sample was prepared by first incubating the purified enzyme under a hydrogen atmosphere for 30 min and then introducing CO directly into the protein solution as described previously.[16,17] The CO-reacted sample was split into a Mössbauer and an EPR sample. Results on the EPR sample have been published previously[17] and showed quantitative (∼1 equiv) development of the axial 2.06 signal.

Mössbauer Measurements. Both the weak-field and strong-field spectrometers operate at a constant acceleration mode in a transmission geometry and have been described elsewhere.[21] The zero velocity refers to the centroid of room-temperature spectra of a metallic iron foil.

Spectral Analysis. Since the paramagnetic Fe−S clusters involved in the current study all have a ground-state spin of $S = {}^1/_2$, their low-temperature Mössbauer spectra can be analyzed by using the following spin Hamiltonian.

$$H_S = \beta \mathbf{S}\cdot\mathbf{g}\cdot\mathbf{H} + \sum_{i=1}^{n} \frac{eQ(V_{zz})_i}{4}\left[\mathbf{I}_{zi}^2 - \frac{I_i(I_i+1)}{3} + \frac{\eta}{3}(\mathbf{I}_{xi}^2 - \mathbf{I}_{yi}^2)\right] + \sum_{i=1}^{n}(\mathbf{S}\cdot\mathbf{A}_i\cdot\mathbf{I}_i - g_n\beta_n\,\mathbf{H}\cdot\mathbf{I}_i) \quad (1)$$

where i represents the ith Fe site and n is the nuclearity of the cluster. For analyzing the spectra of the two dipolar-coupled $[4Fe\text{-}4S]^+$ F clusters, it is necessary to introduce an additional spin−spin coupled term,

$$H_{dipolar} = \mathbf{S}_1\cdot\mathbf{J}_{dp}\cdot\mathbf{S}_2 \quad (2)$$

where $\mathbf{S}_1$ and $\mathbf{S}_2$ are the spins of the reduced F clusters and $S_1 = S_2 = {}^1/_2$, and $\mathbf{J}_{dp}$ represents the dipolar coupling interaction. At high temperatures (above 77 K), the electronic relaxation is fast in comparison to the ^{57}Fe nuclear Lamor precession. Under such conditions, the magnetic hyperfine interactions are canceled and the resulting Mössbauer spectra consist of only quadrupole doublets. Consequently, the high-temperature spectra were analyzed as superpositions of quadrupole doublets.

Results

To facilitate our presentation, the following nomenclature is used to describe the different oxidation states of the H cluster: The H cluster in the aerobically purified enzyme is one-electron more oxidized than the rhombic 2.10 H_{OX} state and is thus designated as H_{OX+1}. The H clusters that display the rhombic 2.06 and 2.10 EPR signals are isoelectronic and are therefore labeled as $H_{OX-2.06}$ and $H_{OX-2.10}$, respectively. To be consistent with the nomenclature used for other Fe hydrogenases, the CO-reacted H cluster that exhibits the axial 2.06 EPR signal is denoted as H_{OX}-CO.[22] The oxidation state of the H cluster in the −350 mV sample is currently unclear (see Discussion) and is tentatively labeled as H_{red}.

The fact that *D. vulgaris* hydrogenase contains three multinuclear Fe−S clusters has resulted in complex Mössbauer spectra that are composed of overlapping spectra arising from the different Fe sites. This complexity is greater in the −110 and −310 mV samples as the H cluster in these samples exists in equilibrium between two different oxidation states. Analysis of such complex spectra is difficult, and a unique solution cannot be obtained by analyzing any one single spectrum alone. We have therefore employed a global analysis approach, in which the entire set of Mössbauer spectra of all five samples recorded over ranges of temperature (4.2−200 K) and applied field (0−8 T) were considered as a whole. Also, to reduce the complexity, it was assumed that the two F clusters have the same parameters and that the parameters describing a particular cluster depend only on its own electronic state and do not depend on the state of other clusters present in the same molecule. With these two assumptions and by using a self-consistent manual iterative approach, a set of parameters that could satisfactorily explain the entire set of spectra was obtained, and the results are presented below. It should be noted that, for clarity, the contribution of the [3Fe-4S] impurity (4% of the total iron absorption) has been removed from all of the spectra presented in this paper.

Due to the complexity of the problem at hand, we would like to first summarize the results of this global analysis by reporting in Table 1 the stoichiometry of the different Fe−S species found in the five Mössbauer samples and in Tables 2 and 3 the characteristic parameters obtained for the F and H clusters, respectively. From Table 1, it can be seen that the Mössbauer quantifications of $H_{OX-2.06}$, $H_{OX-2.10}$ and H_{OX}-CO are in good agreement with previous EPR findings.[9,16,17] To provide a general impression on the quality of this global

(19) Lemon, B. J.; Peters, J. W. *Biochemistry* **1999**, *38*, 12969−12973.
(20) Lemon, B. J.; Peters, J. W. *J. Am. Chem. Soc.* **2000**, *122*, 3793−3794.
(21) Ravi, N.; Bollinger, J. M., Jr.; Huynh, B. H.; Stubbe, J.; Edmondson, D. E. *J. Am. Chem. Soc.* **1994**, *116*, 8007−8014.
(22) Popescu, C. V.; Münck, E. *J. Am. Chem. Soc.* **1999**, *121*, 7877−7884.

Table 2. Spin Hamiltonian Parameters for the Ferredoxin-Type F Clusters in *D. vulgaris* Hydrogenase[a]

state	Fe site[b]	δ (mm/s)	ΔE_Q (mm/s)	η	$A_{xx}/g_n\beta_n$ (T)[c]	$A_{yy}/g_n\beta_n$ (T)[c]	$A_{yy}/g_n\beta_n$ (T)[c]
$[4Fe\text{-}4S]^{2+}$	1	0.44 (3)	1.49 (5)	0.7 (5)			
	2	0.46 (3)	1.30 (5)	−1.0 (3)			
	3	0.45 (3)	1.28 (5)	1.0 (5)			
	4	0.45 (2)	0.64 (3)	0.9 (3)			
$[4Fe\text{-}4S]^{+}$	Fe(III)Fe(II)	0.49 (3)	1.23 (5)	0.2 (4)	−15.3 (15)	−26.0 (20)	−23.4 (15)
	Fe(II)Fe(II)	0.62 (3)	2.17 (5)	0.0 (4)	19.0 (10)	9.4 (10)	5.0 (10)

[a] Values in parentheses are uncertainties in units of the least significant digit. [b] In our analysis, the $[4Fe\text{-}4S]^{+}$ cluster is assumed to consist of a valence-delocalized Fe(III)Fe(II) pair and a diferrous pair. [c] For comparison with ENDOR data, $A = 1$ MHz is equivalent to $A/g_n\beta_n = 0.73$ T.

Table 3. Spin Hamiltonian Parameters for the H Cluster in *D. vulgaris* Hydrogenase[a]

oxidation state	subcluster	Fe site[b]	δ (mm/s)	ΔE_Q (mm/s)	η	$A_{xx}/g_n\beta_n$ (T)[c]	$A_{yy}/g_n\beta_n$ (T)[c]	$A_{zz}/g_n\beta_n$ (T)[c]
H_{OX+1}	$[4Fe\text{-}4S]_H^{2+}$	Pair 1	0.47 (3)	1.24 (5)	−0.5			
		Pair 2	0.44 (3)	0.82 (5)	1.0			
	$[2Fe]_H$	Fe1 & Fe2	0.16 (4)	1.09 (5)	0.4			
$H_{OX-2.06}$	$[4Fe\text{-}4S]_H^{+}$	Fe(III)Fe(II)	0.49 (3)	1.12 (5)	−0.3	−19.9 (10)	−26.8 (15)	−22.3 (10)
		Fe(II)Fe(II)	0.57 (3)	−2.30 (5)	1.4	15.7 (10)	9.5 (7)	17.5 (15)
	$[2Fe]_H$	Fe1 & Fe2	0.17 (4)	1.08 (5)	0.4			
$H_{OX-2.10}$	$[4Fe\text{-}4S]_H^{2+}$	Pair 1	0.44 (3)	1.14 (10)	0.0	−6.2 (7)	−6.2 (7)	−6.2 (7)
		Pair 2	0.43 (3)	1.34 (10)	−0.8	6.2 (10)	6.2 (10)	6.2 (10)
	$[2Fe]_H$	Fe1	0.13 (4)	0.85 (6)	0.0	0	0	0
		Fe2	0.14 (3)	0.67 (6)	0.0	−12.0 (5)	−12.0 (5)	−12.0 (5)
H_{OX}-CO	$[4Fe\text{-}4S]_H^{2+}$	Pair 1	0.44 (3)	0.95 (5)	0.8	−23.5 (20)	−28.0 (20)	−22.6 (20)
		Pair 2	0.41 (3)	0.98 (5)	−1.0	23.0 (10)	21.5 (10)	20.4 (10)
	$[2Fe]_H$	Fe1	0.17 (3)	0.70 (5)	0	−5.0 (15)	−5.0 (15)	−5.0 (15)
		Fe2	0.13 (3)	0.65 (5)	−1.0	0	0	0
H_{red}	$[4Fe\text{-}4S]_H^{2+}$	Pair 1	0.47 (3)	1.24 (5)	−0.5			
		Pair 2	0.44 (3)	0.82 (5)	1.0			
	$[2Fe]_H$	Fe1 & Fe2	0.13 (4)	0.85 (6)	0.0			

[a] Values in parentheses are uncertainties in units of the least significant digit. [b] In our analysis, the $[4Fe\text{-}4S]_H^{2+}$ subcluster is assumed to consist of two Fe(III)Fe(II) pairs and the $[4Fe\text{-}4S]^{+}$ is assumed to consist of an Fe(III)Fe(II) pair and a diferrous pair. [c] $A = 1$ MHz is equivalent to $A/g_n\beta_n = 0.73$ T.

analysis, we show in Figure 2 a representative set of the Mössbauer spectra (hashed marks) of the five samples recorded at 4.2 K with a parallel field of 0.05 T in comparison with the results of our analysis which are plotted over the experimental data as solid lines. The agreement between the experimental spectra and the theoretical simulations is excellent. In the following, major observations and results obtained from the global analysis are described for each sample.

The As-purified Enzyme. The 4.2 K Mössbauer spectrum of the aerobically purified enzyme recorded in the presence of a parallel applied field of 0.05 T displays a broad and unresolved quadrupole doublet (Figure 2A) arising from the two $[4Fe\text{-}4S]^{2+}$ F clusters and the H_{OX+1} cluster. Spectra recorded in strong applied fields (data not shown) indicate that both the F and the H clusters in the as-purified enzyme are diamagnetic. As the spectra of these two types of clusters are unresolved, a unique deconvolution of the spectra of the as-purified enzyme is not possible without considering the spectra of other samples (i.e., global analysis is required). In this particular case, it was useful to consider the spectra of the −110 mV sample in which part of the H clusters have been reduced to the $H_{OX-2.06}$ state while the F clusters remain in the $[4Fe\text{-}4S]^{2+}$ state. Taking a difference between spectra A and B of Figure 2, in principle, would cancel the contributions from the F clusters and thus generate a spectrum (Figure 3) that reveals changes occurred at the H cluster.[23] The downward pointing quadrupole doublet is arising from the H_{OX+1} cluster, and the upward pointing magnetic spectrum represents the $H_{OX-2.06}$ cluster. In the next section, we will present arguments supporting that this difference spectrum represents changes that occur on the $[4Fe\text{-}4S]_H$ subcluster and not on the binuclear $[2Fe]_H$ subcluster. The downward pointing doublet is thus arising from the $[4Fe\text{-}4S]_H$ cluster and can be analyzed as a superposition of two quadrupole doublets. The resulting parameters are listed in Table 3. These parameters together with the observed diamagnetism indicate that the $[4Fe\text{-}4S]_H$ subcluster in the H_{OX+1} cluster is in the 2+ oxidation state. With the parameters for the $[4Fe\text{-}4S]_H^{2+}$ cluster determined, it becomes possible to decompose the spectra of the as-purified enzyme and to obtain characteristic parameters for the F clusters and the $[2Fe]_H$ subcluster. The results obtained for the F clusters are typical for a ferredoxin-like $[4Fe\text{-}4S]^{2+}$ cluster and can be used for analysis of the spectra of the −110 mV sample, which contains F clusters at the same oxidation state. In practice, the final parameters are obtained by iterative executions of the analysis steps outlined above until a set of parameters is found to be consistent with the spectra of both the as-purified and −110 mV samples.

At high-temperatures, the spectrum of the $[2Fe]_H$ cluster is partially resolved from the major spectral components, and therefore the parameters for the $[2Fe]_H$ subcluster obtained from the 4.2 K spectrum (Figure 2A) may be confirmed by the high-temperature spectra. Figure 4 shows a 190-K spectrum of the as-purified enzyme recorded in the absence of an applied field. A shoulder at ∼−0.5 mm/s (indicated by an arrow) is observed. This shoulder is assigned to the low-energy line of the quadrupole doublet originating from the $[2Fe]_H$ subcluster. The

(23) In practice, the spectrum of the F clusters in the as-purified enzyme was found to be slightly broader than that of the F clusters in the −110 mV sample, resulting in the small sharp peaks observed at −0.5 and +1.3 mm/s in the difference spectrum (Figure 3). This broadening may indicate a slightly less defined environment for the F clusters in the as-purified enzyme. The major features in the difference spectrum, however, are not affected by this minor difference in the F clusters between the two samples.

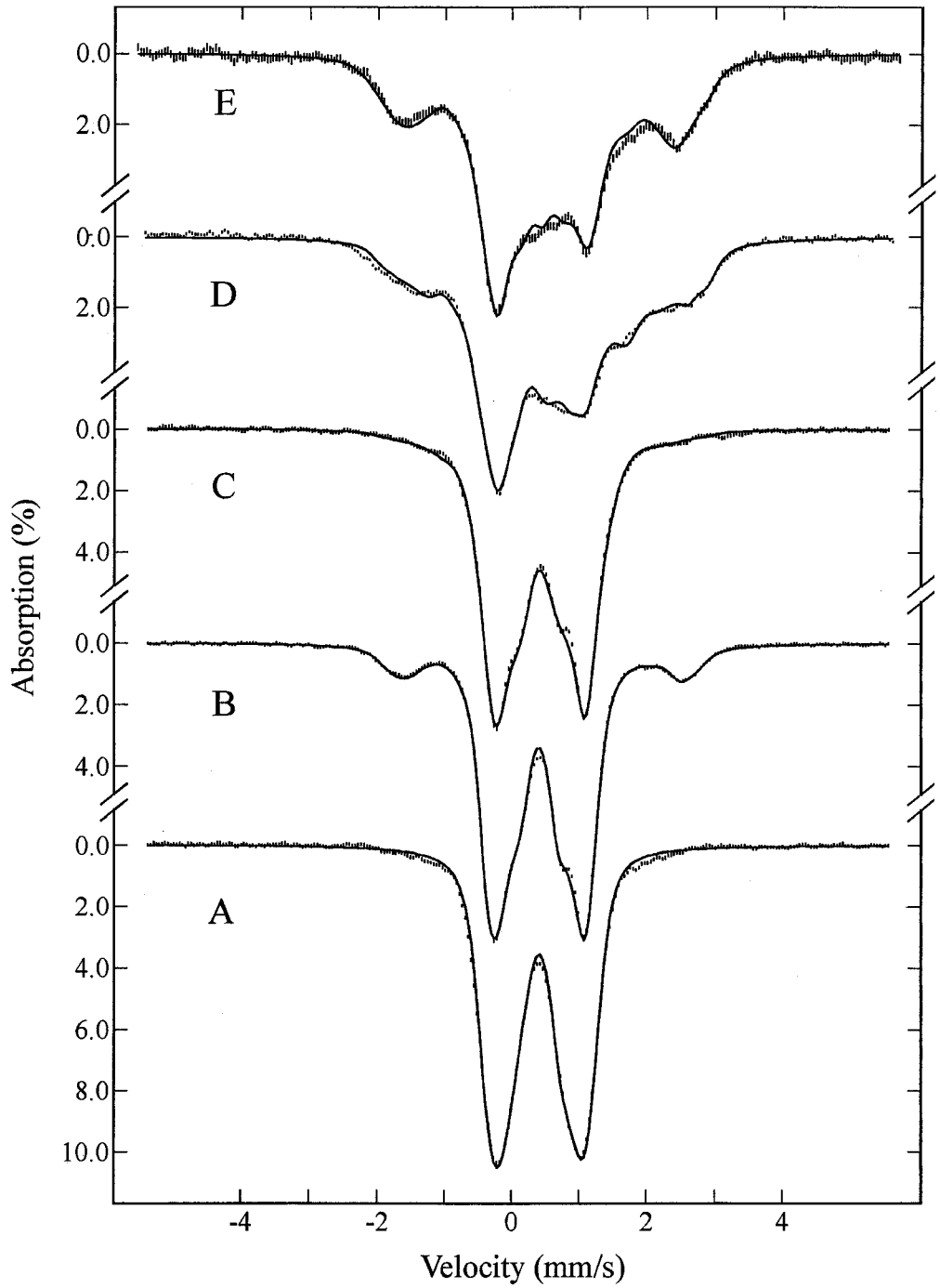

Figure 2. Mössbauer spectra of *D. vulgaris* hydrogenase at various oxidation states generated during reductive activation (A, as purified; B, −110 mV; C, −310 mV; and D, −350 mV), and after reacting the reduced enzyme with CO (E). The experimental spectra (hashed marks) are recorded at 4.2 K in a 0.05 T magnetic field applied parallel to the γ beam. The solid lines are theoretical simulations using the parameters listed in Tables 1−3.

fact that it is partially resolved from the spectra of the [4Fe-4S]$^{2+}$ F clusters and [4Fe-4S]$_H^{2+}$ subcluster at high temperatures is because [4Fe-4S]$^{2+}$ cluster exhibits temperature-dependent quadrupole splitting (decreasing ΔE_Q with increasing temperature), while the Fe sites of the [2Fe]$_H$ subcluster, with the strong CO and CN ligand, are low-spin and exhibit relatively temperature-independent quadrupole splitting. Least-squares fitting the 190-K spectrum with three quadrupole doublets, a minor doublet representing the [2Fe]$_H$ cluster and two major doublets representing the [4Fe-4S]$^{2+}$ clusters, yields $\Delta E_Q = 1.16$ mm/s and $\delta = 0.07$ mm/s for the minor doublet, and $\Delta E_Q(1) = 0.55$ mm/s, $\delta(1) = 0.35$ mm/s, $\Delta E_Q(2) = 0.90$ mm/s and $\delta(2) = 0.37$ mm/s for the major doublets. The minor doublet accounts for 14.3% of the total Fe absorption, while the major doublets 1 and 2 account for 29 and 56.7%, respectively. The parameters for the minor doublet are consistent with those of the [2Fe]$_H$ obtained at 4.2 K, and the parameters for the major doublets are indicative of [4Fe-4S]$^{2+}$ clusters. Most importantly, the fit indicates the minor doublet (shown as a dashed line in Figure 4) contributes ∼14% of the total iron absorption. Since *D. vulgaris* hydrogenase contains a total of 14 Fe atoms/molecule, the 14% contribution corresponds to two Fe atoms, consistent with the assignment of the minor doublet to the [2Fe]$_H$ subcluster. The observation of a single doublet for the [2Fe]$_H$

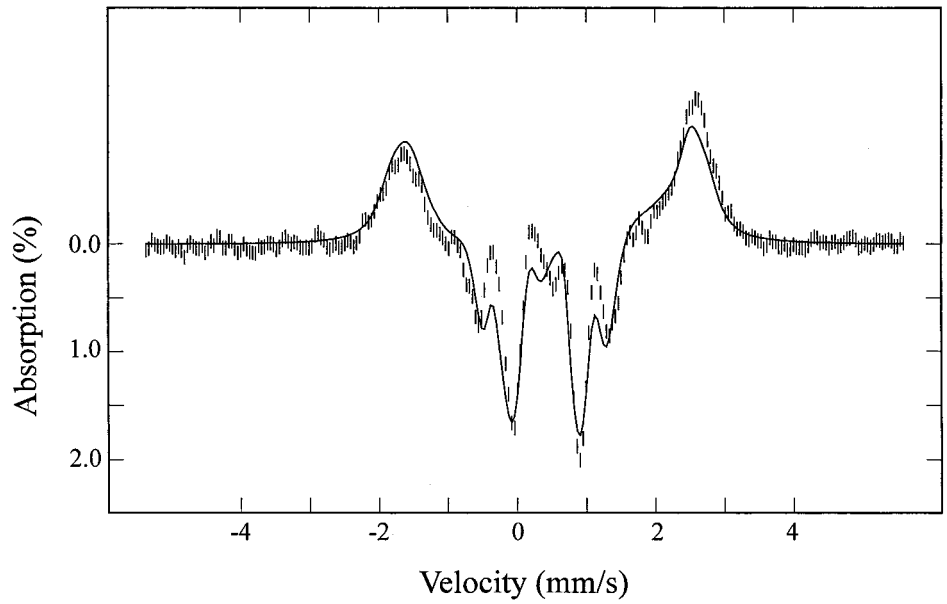

Figure 3. Difference spectrum of spectra A and B shown in Figure 2, demonstrating the spectral changes observed between the aerobically purified hydrogenase and the enzyme poised at −110 mV. The solid line is a theoretical difference spectrum between the simulated spectra of the as-purified and −110 mV samples using the parameters listed in Table 3.

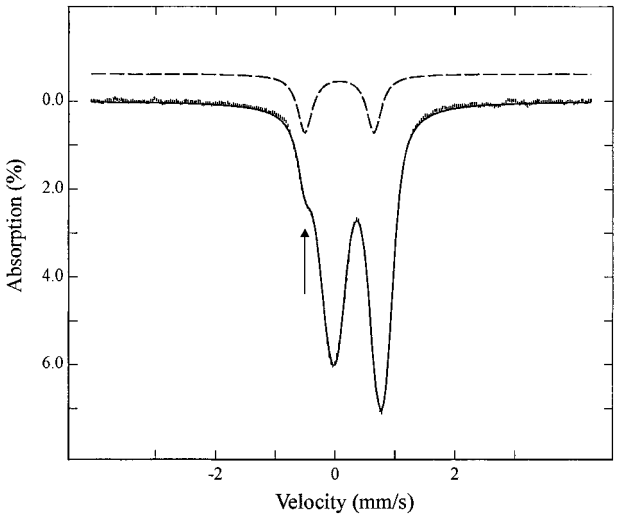

Figure 4. Mössbauer spectrum of the −110 mV sample recorded at 190 K in the absence of a magnetic field. The solid line is a least-squares fit to the data assuming three quadrupole doublets (see text for parameters). The dashed line shows the quadupole doublet that represents the $[2Fe]_H$ subcluster.

also indicates that the two iron sites in H_{OX+1} are indistinguishable by Mössbauer spectroscopy. Because of the unusual coordination environment of the $[2Fe]_H$ and the lack of data on suitable model compounds, the oxidation state of the Fe cannot be definitely inferred from the Mössbauer parameters (see Discussion). As the enzyme was purified aerobically, it is likely that the two Fe atoms may be in the ferric state. However, the parameters obtained for the $[2Fe]_H$ cluster ($\Delta E_Q = 1.09$ mm/s and $\delta = 0.16$ mm/s) are very similar to those ($\Delta E_Q = 0.91$ mm/s and $\delta = 0.15$ mm/s) reported for a low-spin ferrous compound $[Fe^{II}(PS3)(CO)(CN)]^{2-}$ with similar ligand environment,[24] suggesting that a diferrous assignment may also be possible.

The −110 mV Sample. The Mössbauer spectrum of the −110 mV sample recorded at 4.2 K in a parallel field of 0.05 T (Figure 2B) displays a central broad quadrupole doublet and a magnetic spectrum with absorption extending between −2 and +2.5 mm/s. Since the sample exhibits only one EPR signal, namely, the rhombic 2.06 signal, the magnetic spectrum is assigned to the $H_{OX-2.06}$ species. As mentioned above, the difference spectrum (Figure 3) between spectra A and B of Figure 2 reveals spectral changes caused by the one-electron reduction of H_{OX+1} to $H_{OX-2.06}$. The fact that the characteristic quadrupole doublet of $[2Fe]_H$ in H_{OX+1} is not observed in the difference spectrum indicates that the $[2Fe]_H$ cluster remains at the same electronic state during H_{OX+1} to $H_{OX-2.06}$ reduction. Detailed analysis of the spectrum of the −110 mV sample (Figure 2B) shows that the magnetic component contributes about 18% of the total iron absorption, a value corresponding to 2.5 Fe atoms or 0.63 equiv of a [4Fe-4S] cluster. These observations together with the EPR quantification of 0.7 equiv of the rhombic 2.06 species strongly suggest that the reduction of H_{OX+1} to $H_{OX-2.06}$ occurs at the $[4Fe\text{-}4S]_H$ subcluster. Detailed analysis of the field dependence of the magnetic component supports this suggestion.

Figure 5 shows the 4.2 K spectra of the magnetic component (hashed marks) recorded in a parallel applied field of 0.05 T (A), 2 T (B), 4 T (C), 6 T(D), or 8 T (E). These spectra are prepared by removing the contributions of the diamagnetic $[2Fe]_H$ subcluster, F clusters, and 0.37 equiv of the $[4Fe\text{-}4S]_H^{2+}$ subcluster from the raw data using theoretical spectra simulated with the parameters listed in Tables 2 and 3. With increasing field strength, one outward moving spectral component and one inward moving component are clearly discernible. The observed magnetic splitting and field dependence are typical for $[4Fe\text{-}4S]^+$ clusters, of which the Mössbauer spectra consist of two subspectra representing a valence-delocalized Fe(II)Fe(III) pair and a diferrous pair.[25,26] Analysis of the magnetic spectra shown in Figure 5 yielded the parameters listed in Table 3, and the resulting theoretical spectra are shown in Figure 5 as solid lines. Consistent with the assignment that the $[4Fe\text{-}4S]_H$ subcluster has been reduced to the 1+ state, the parameters are charac-

(24) Hsu, H.-F.; Koch, S. A.; Popescu, C. V.; Münck, E. *J. Am. Chem. Soc.* **1997**, *119*, 8371−8372.

(25) Middleton, P.; Dickson, D. P. E.; Johnson, C. E.; Rush, J. D. *Eur. J. Biochem.* **1978**, *88*, 135−41.

(26) Trautwein, A. X.; Bill, E.; Bominaar, E. L.; Winkler, H. *Struct. Bonding (Berlin)* **1991**, *78*, 1−95.

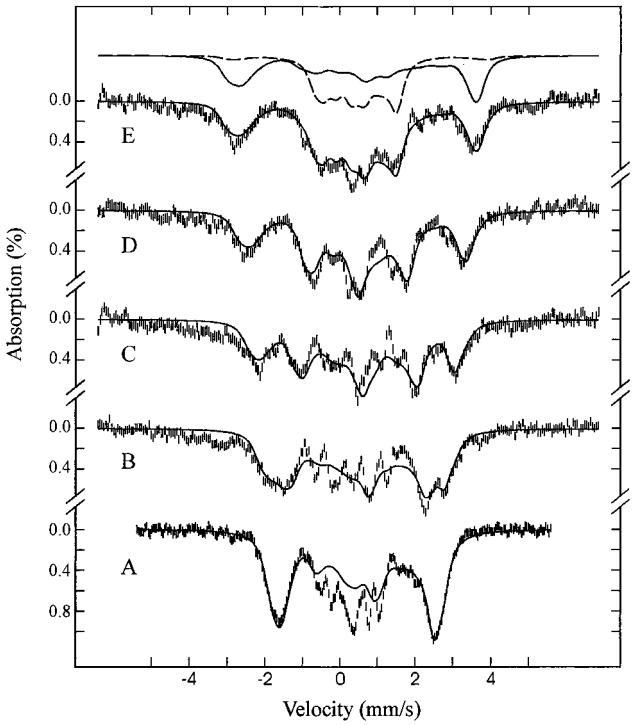

Figure 5. Field-dependent Mössbauer spectra of $[4Fe\text{-}4S]_H^+$ subcluster of $H_{OX-2.06}$. The data were recorded at 4.2 K in a parallel applied field of 0.05 T (A), 2 T (B), 4 T (C), 6 T (D), or 8 T (E). These spectra were prepared from the spectra of the −110 mV sample by removing the contributions of other species from the raw data using theoretical spectra simulated with parameters listed in Tables 1−3. The solid lines overlaid with the experimental spectra are theoretical simulations using the parameters listed in Table 3. For the 8 T spectrum, individual spectral components representing the diferrous pair and the valence-delocalized Fe(III)Fe(II) pair are also shown above spectrum E as a solid and a dashed line, respectively.

teristics of ferredoxin like $[4Fe\text{-}4S]^+$ clusters.[25,26] Similar to other $[4Fe\text{-}4S]^+$ clusters, the outward moving component (positive A value) has larger magnitude of ΔE_Q (2.30 mm/s) and isomer shift ($\delta = 0.57$ mm/s) representing the diferrous pair, and the inward moving component (negative A value) has smaller ΔE_Q (1.12 mm/s) and isomer shift ($\delta = 0.49$ mm/s) representing the mixed valence pair. Consequently, on the basis of the Mössbauer data, it can be concluded that the $H_{OX-2.06}$ state is one electron further reduced from the H_{OX+1} and that the reducing equivalent is localized on the $[4Fe\text{-}4S]_H$ subcluster.

The −310 mV sample. Comparing the Mössbauer spectrum of the −310 mV sample recorded at 4.2 K in a parallel field of 0.05 T (Figure 2C) with that of the −110 mV sample recorded under the same experimental conditions (Figure 2B) shows that, except for the weak shoulders observed at −1.5 and +2.7 mm/s, no other magnetic spectral component with a splitting comparable to that of $H_{OX-2.06}$ is detected in the spectrum of the −310 mV sample. On the basis of the EPR data,[9] which showed partial reduction of the F clusters in the −310 mV sample, and in comparison with the Mössbauer spectrum of the −350 mV sample (Figure 2D), which contains fully reduced F clusters, the shoulders observed at −1.5 and +2.7 mm/s are assigned to the reduced $[4Fe\text{-}4S]^+$ F clusters. Consequently, the magnetic spectrum arising from the $H_{OX-2.10}$ species must have a magnetic hyperfine splitting that is smaller than that of $H_{OX-2.06}$ so that the $H_{OX-2.10}$ spectrum is overlapping with the central quadrupole doublet. In other words, the magnetic hyperfine interaction for the $H_{OX-2.10}$ species is much smaller than that of the $H_{OX-2.06}$ species. This is not surprising since

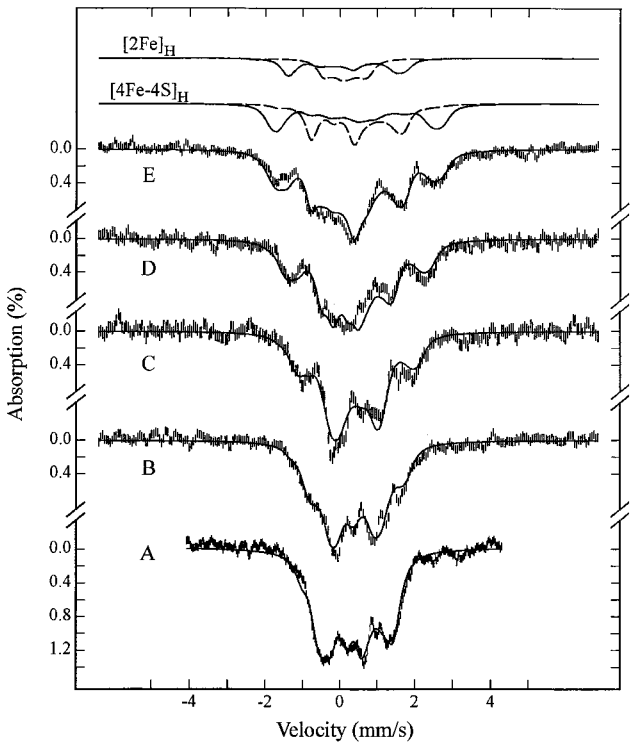

Figure 6. Field-dependent Mössbauer spectra of $H_{OX-2.10}$. The data were recorded at 4.2 K in a parallel applied field of 0.05 T (A), 2 T (B), 4 T (C), 6 T (D), or 8 T (E). These spectra were prepared from the spectra of the −310 mV sample by removing the contributions of other species from the raw data using theoretical spectra simulated with parameters listed in Tables 1−3. The solid lines overlaid with the experimental spectra are theoretical simulations using the parameters of $H_{OX-2.10}$ listed in Table 3. For the 8 T spectrum, individual spectral components originating from the Fe sites of the $[2Fe]_H$ subcluster (Fe1: solid line, Fe2: dashed line) and $[4Fe\text{-}4S]_H^{2+}$ cluster (pair 1: dashed line, pair 2: solid line) are also shown above spectrum E.

ENDOR studies on the $H_{OX-2.10}$ species of *C. pasteurianum* hydrogenases I and II showed two ^{57}Fe resonances corresponding to magnetic hyperfine coupling A values of ∼12−13 and 5−7 T (17−18 and 7−9.5 MHz, respectively),[27,28] which are about half of the magnitudes of the A values determined for $H_{OX-2.06}$ (see Table 3). Consistent with the ENDOR findings, Mössbauer spectra with small magnetic hyperfine splittings have been observed for the $H_{OX-2.10}$ species in the *C. pasteurianum* hydrogenases.[22,27]

Global analysis of the Mössbauer data of all the *D. vulgaris* hydrogenase samples indicates that in the −310 mV sample, 0.5 equiv of the H cluster is in the $H_{OX-2.10}$ state. Figure 6 shows the 4.2-K field-dependent spectra (hashed marks) of $H_{OX-2.10}$ prepared from the spectra of the −310 mV sample by removing the contributions of other species using the parameters listed in Tables 2 and 3. These spectra can be analyzed as originating from four distinct iron sites: two for the $[2Fe]_H$ subcluster, each site representing one Fe atom, and two for the $[4Fe\text{-}4S]_H$ subcluster, each site representing a diiron pair. The parameters obtained for the four iron sites are listed in Table 3 and the solid lines overlaying the experimental data are theoretical simulations using these listed parameters. Theoretical simulations for the individual Fe sites are also plotted above the 8-T spectrum (Figure 6E). The magnetic hyperfine coupling A values

(27) Wang, G.; Benecky, M. J.; Huynh, B. H.; Cline, J. F.; Adams, M. W. W.; Mortenson, L. E.; Hoffman, B. M.; Münck, E. *J. Biol. Chem.* **1984**, *259*, 14328−14331.

(28) Telser, J.; Benecky, M. J.; Adams, M. W. W.; Mortenson, L. E.; Hoffman, B. M. *J. Biol. Chem.* **1987**, *262*, 6589−6594.

determined for the four Fe sites are consistent with the ENDOR findings for the *C. pasteurianum* hydrogenases[27,28] and indicate that the ENDOR resonance corresponding to the smaller magnitude of A (5−7 T) is originating from the $[4Fe\text{-}4S]_H$ subcluster, while the resonance corresponding to the larger A value (12−13 T) is originating from one of the Fe atoms of the $[2Fe]_H$ subcluster. The same conclusion has been reached from a Mössbauer investigation on the *C. pasteurianum* hydrogenase II.[22] In fact, the Mössbauer parameters obtained for $H_{OX-2.10}$ of *D. vulgaris* hydrogenase are very similar to those reported for the *C. pasteurianum* hydrogenase II. In the case of the *C. pasteurianum* hydrogenase, the data were explained by the coupling of a $[4Fe\text{-}4S]_H^{2+}$ cluster to an $S = {}^1/_2$ $[2Fe]_H$ subcluster.[22] The same argument is applied here and is presented below.

The isomer shifts ($\delta = 0.44$ and 0.43 mm/s) obtained for the diiron pairs suggest that the $[4Fe\text{-}4S]_H$ subcluster is in the 2+ state. Since $[4Fe\text{-}4S]^{2+}$ clusters generally have diamagnetic ground states, the observation of magnetic hyperfine interactions associated with the diiron pairs indicates that the $[4Fe\text{-}4S]_H$ subcluster is not magnetically isolated and must be coupled to a paramagnetic species. Further, the signs and magnitudes of the detected magnetic hyperfine A values can be explained by a theoretical model that assumes a $[4Fe\text{-}4S]^{2+}$ cluster exchange coupled via one of its Fe atom to an $S = {}^1/_2$ center.[22,29,30] In this model, the $[4Fe\text{-}4S]^{2+}$ cluster is assumed to consist of two $S = {}^9/_2$ mixed-valence Fe(II)Fe(III) pairs. The pairs are antiferromagnetically coupled to form a diamagnetic ground state and an $S = 1$ first excited state. Exchange coupling (coupling constant j) between the $S = {}^1/_2$ center and one of the corner Fe of the [4Fe-4S] cube mixes the excited $S = 1$ state of the cube into its diamagnetic ground state, resulting in the observed magnetic interactions on the [4Fe-4S] cube. Consequently, according to this model, the magnitudes of the induced magnetic hyperfine interactions should depend on the ratio of the coupling constant j and the energy separation Δ between the ground and first excited state of the cube: the larger the j/Δ ratio, the more mixing of the excited-state resulting in the greater magnitudes of the magnetic hyperfine interactions. Figure 7 shows the induced A values for the two Fe(II)Fe(III) pairs as functions of j/Δ, calculated by using eq 3 of Xia et al.[30] The observed A values ($\pm$ 6.2 T) for the two mixed-valence pairs of the $[4Fe\text{-}4S]_H$ cluster are reproduced with a $j/\Delta = 0.1$. For the $[2Fe]_H$ subcluster, one Fe site exhibits magnetic hyperfine interaction, while the other is diamagnetic. Taking into consideration the ligand environment and the above-described theoretical model, the magnetic Fe site must associated with the $S = {}^1/_2$ center that is coupled to the $[4Fe\text{-}4S]_H$ subcluster. Thus, this Fe site is assigned to a low-spin Fe(III) or Fe(I) ($S = {}^1/_2$). The diamagnetic Fe site is then assigned to a low-spin Fe(II) ($S = 0$). In other words, for $H_{OX-2.10}$ the reducing equivalent is localized on the $[2Fe]_H$ subcluster, in contrast to $H_{OX-2.06}$, in which the reducing equivalent is localized on the $[4Fe\text{-}4S]_H$ subcluster (see Discussion).

The −350 mV Sample. In the −350 mV sample, both F clusters are reduced to the $S = {}^1/_2$ $[4Fe\text{-}4S]^+$ state. Previous EPR investigation indicated that the two reduced F clusters are weakly spin−spin coupled.[8] This weak coupling is also revealed in the field-dependent Mössbauer spectra of the reduced F clusters (Figure 8) prepared from the spectra of the −350 mV sample by removing the contributions of the H cluster using the parameters listed in Table 3. In Figure 8, the experimental

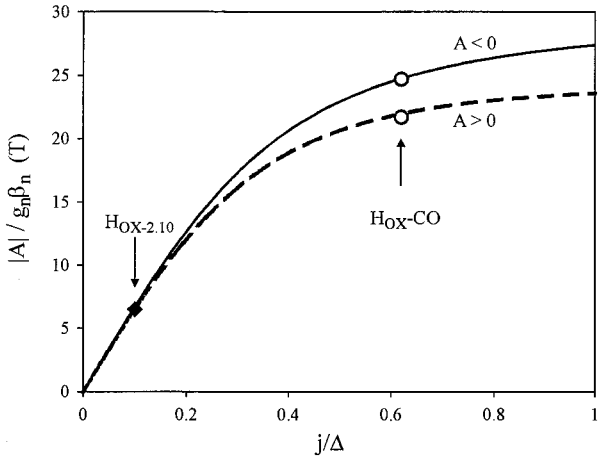

Figure 7. Absolute values of the induced magnetic hyperfine coupling constants for the two valence-delocalized Fe(III)Fe(II) pairs of a $[4Fe\text{-}4S]^{2+}$ cluster in a spin coupled $\{[4Fe\text{-}4S]^{2+}-Fe\ (S = {}^1/_2)\}$ system[29] as functions of j/Δ calculated from eq 3 of Xia et al.[30] An intrinsic magnetic hyperfine coupling constant of $a/g_n\beta_n = 16$ T was used in this calculation. The black diamond shows the value obtained for $H_{OX-2.10}$, and the circles indicate the values obtained for the two pairs in H_{OX}-CO.

spectra (hashed marks) of the reduced F clusters are presented in duplicate for comparison with theoretical simulations with (panel B) and without (panel A) the assumption of spin−spin coupling. In panel A, the theoretical spectra (solid lines) are simulated using the parameters listed in Table 2 and with the assumption that the F clusters are magnetically isolated (i.e., no coupling). The simulations agree well with experimental data recorded in magnetic fields ≥ 1 T and disagree with the spectrum recorded in 0.05 T. This observation is consistent with the presence of a weak coupling that can be decoupled by the application of a moderate field (e.g., 1 T). Using the distance between the two F clusters (11.8 Å) determined from the crystallographic data,[11] a dipolar coupling on the order of 1×10^{-3} cm^{-1} is estimated between the two $S = {}^1/_2$ clusters. Including a coupling of this magnitude in our analysis (see Methods) yielded theoretical spectra (Figure 8, panel B, solid lines) in agreement with experimental data recorded at all fields, including the 0.05 T spectrum.

Removing the contributions of the F clusters from the raw data, by using the theoretical simulations of the F clusters presented above, yields spectra representing the H_{red} cluster (Figure 9). These spectra can be decomposed into three spectral components with parameters listed in Table 3. The weak-field spectrum (Figure 9A) can be explained as a sum of three quadrupole doublets, and the strong-field spectrum (Figure 9B) can be simulated with same parameters of the three doublets and assuming diamagnetism, indicating that the ground electronic state of H_{red} is diamagnetic. Two of the doublets are assigned to the two diiron pairs of the $[4Fe\text{-}4S]_H$ cluster and the remaining doublet to the $[2Fe]_H$ cluster. For the $[4Fe\text{-}4S]_H$ subcluster, the parameters are characteristic for $[4Fe\text{-}4S]^{2+}$ state. For the $[2Fe]_H$ subcluster, the parameters are identical to those of the low-spin ferrous site in $H_{OX-2.10}$. On the other hand, the diamagnetism and parameters observed for H_{red} are very similar to those of H_{OX+1}, making it ambiguous in defining the oxidation state of the $[2Fe]_H$ subcluster based solely on Mössbauer parameters (also see Discussion).

The CO-Reacted Sample. The 4.2-K 0.05-T spectrum of the CO-reacted sample (Figure 2E) shows substantial magnetic contributions that are comparable to that of the −350 mV sample, in which the two F clusters are in the paramagnetic

(29) Belinsky, M. I. *J. Biol. Inorg. Chem.* **1996**, *1*, 186−188.
(30) Xia, J.; Hu, Z.; Popescu, C. V.; Lindahl, P. A.; Münck, E. *J. Am. Chem. Soc.* **1997**, *119*, 8301−8312.

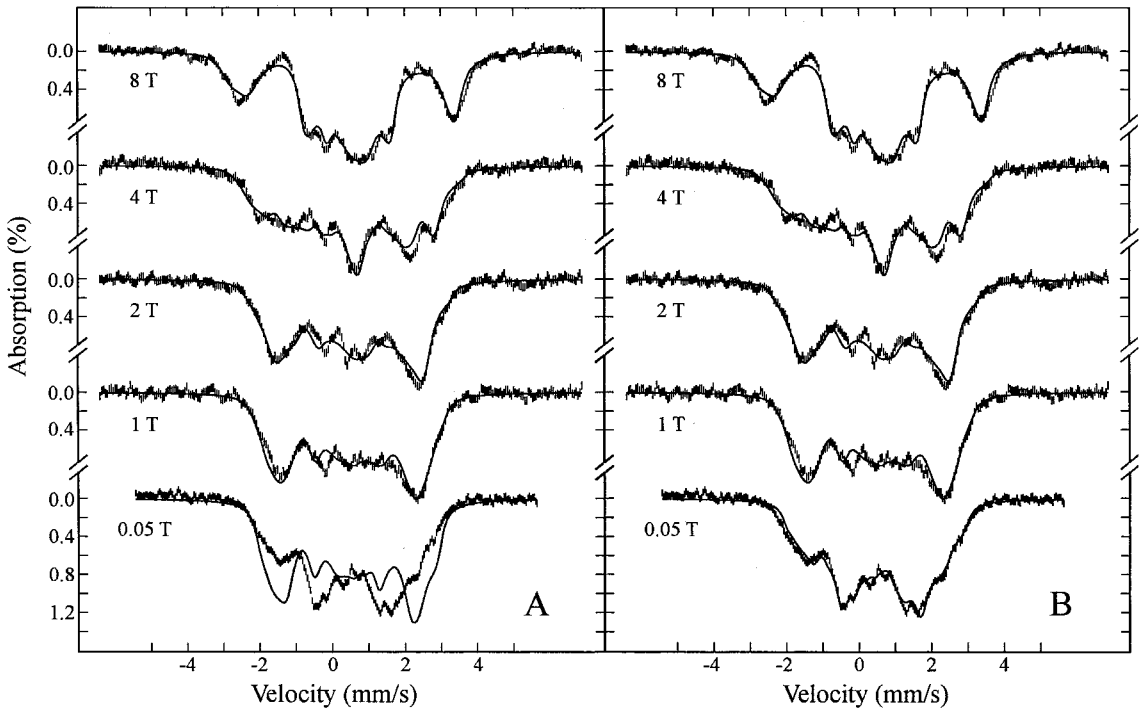

Figure 8. Field-dependent Mössbauer spectra of the two weakly interacting [4Fe-4S]$^{+}$ F clusters. These spectra are prepared from the spectra of the −350 mV sample by removing the contribution of the H cluster from the raw data using theoretical spectra simulated with the parameters of H_{red} listed in Table 3. The data were recorded at 4.2 K in fields as indicated in the Figure. Each spectrum is shown in duplicate in panels A and B for comparison with theoretical spectra (solid lines) simulated with the absence of magnetic coupling between the two F clusters (Panel A) and with the presence of a coupling constant of 1×10^{-3} cm^{-1} (Panel B). In principle, dipolar coupling is axially symmetric. In this case, however, the coupling is weak, and the symmetry of the coupling interaction has an insignificant effect on the simulated spectra.

[4Fe-4S]$^{+}$ state. This observation indicates that (1) the H_{OX}-CO cluster must exhibit a spectrum with magnetic splitting comparable to that of the [4Fe-4S]$^{+}$ F cluster, and (2) a portion of the F clusters must be reduced. Detailed analysis of the Mössbauer data recorded under different experimental conditions indicates that, in the CO-treated sample, nearly all of the H clusters have reacted with CO forming the H_{OX}-CO clusters and approximately 0.9 equiv of the F clusters is in the 1+ state. Figure 10 shows the field-dependent Mössbauer spectra of H_{OX}-CO prepared by removing contributions of other species from the spectra of the CO-reacted sample (a weak coupling of 10^{-3} cm^{-1} between the [4Fe-4S]$^{+}$ F clusters was assumed in the simulation of the theoretical spectrum used to remove the contributions of the reduced F clusters). Similar to $H_{OX-2.10}$, the spectra of H_{OX}-CO can also be decomposed into four components, two representing the two Fe sites of the $[2Fe]_H$ subcluster and the other two representing two diiron pairs in the $[4Fe\text{-}4S]_H$ subcluster. The resulting parameters for the four Fe sites are listed in Table 3, and the theoretical simulations using these parameters are plotted in Figure 10 as solid lines. The isomer shifts obtained for the two Fe pairs are consistent with mixed-valence Fe(II)Fe(III) pairs and suggest [4Fe-4S]$^{2+}$ state for the $[4Fe\text{-}4S]_H$ subcluster. The observed magnetic hyperfine interactions for this $[4Fe\text{-}4S]_H^{2+}$ cluster, again, can be explained by the theoretical model used for $H_{OX-2.10}$ and corresponding to a much larger j/Δ value of ∼0.62 (see Figure 7). The magnetic hyperfine A value (−5 T) determined for the paramagnetic Fe site of the $[2Fe]_H$ subcluster of H_{OX}-CO, on the other hand, is substantially smaller in magnitude than the value (−12 T) found for that of $H_{OX-2.10}$. This reduction in the magnitude of A can also be explained qualitatively by the same theoretical model and is correlated with the increase in j/Δ. According to this model, induction of paramagnetism in the diamagnetic cube reduces the magnetic hyperfine A value at the $S = {}^1/_2$ Fe site given by eq 3,[29]

$$A = a\left[1 + \frac{2(1-x)}{\Gamma}\right]\frac{1}{3} \qquad (3)$$

where a is the intrinsic magnetic hyperfine constant for the $S = {}^1/_2$ Fe site, $x = j/(4\Delta)$ and $\Gamma = (1 - 2x + 100x^2)^{1/2}$. According to eq 3, the apparent A value approaches the intrinsic a value for small j/Δ. Since the j/Δ ratio is small for $H_{OX-2.10}$, we may assume the value −12 T obtained for the paramagnetic Fe site in $H_{OX-2.10}$ to be the intrinsic a value. Using $a = -12$ T and $j/\Delta = 0.62$, eq 3 yields an A value of −7.8 T, representing a substantial reduction in the magnitude of the A value for the paramagnetic Fe site.

Discussion

Reductive Activation of Aerobically Purified *D. vulgaris* Hydrogenase. Although the aerobically purified *D. vulgaris* hydrogenase is stable in air, it is inactive and requires reductive activation. Once reduced, the enzyme becomes sensitive to O_2. Previous EPR investigations[7,9] have shown that this reductive process is associated with the conversion of a species that exhibits a rhombic 2.06 EPR signal to a distinct species that exhibits a rhombic 2.10 signal (termed $H_{OX-2.06}$ and $H_{OX-2.10}$ in this paper, respectively). Both signals were assigned to the catalytic H cluster, and the conversion was proposed to reflect an irreversible conformational change rather than a two-electron reduction on the H cluster.[9] In this manuscript, we have used Mössbauer spectroscopy to investigate samples of *D. vulgaris* hydrogenase prepared during reductive activation, and have obtained characteristic parameters for both $H_{OX-2.06}$ and $H_{OX-2.10}$. The results indicate that $H_{OX-2.06}$ and $H_{OX-2.10}$ are isoelectronic. Both are one-electron further reduced from the H_{OX+1} state of the H cluster in the as-purified enzyme. Thus, the Mössbauer

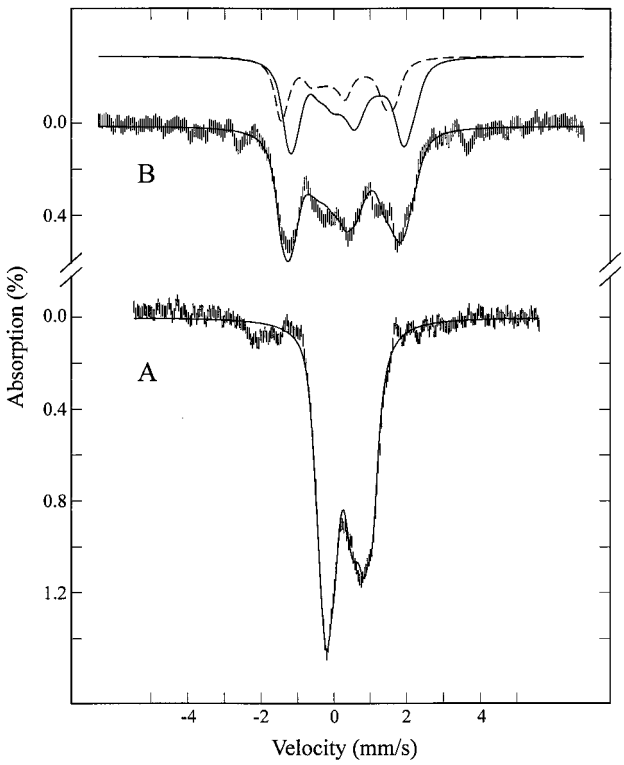

Figure 9. Field-dependent Mössbauer spectra of H_{red}. The data were recorded at 4.2 K in a parallel field of 0.05 T (A) or 8 T (B). These spectra were prepared from the spectra of the −350 mV sample by removing the contributions of the F clusters from the raw data using theoretical spectra simulated with the parameters listed in Table 2. For simulations of the reduced $[4Fe\text{-}4S]^+$ F clusters, a weak spin−spin interaction of 10^{-3} cm^{-1} was assumed. The solid lines overlaid with the experimental data are simulations of H_{red} using the parameters listed in Table 3 and assuming diamagnetism. For the 8 T spectrum (B), theoretical simulations for the $[4Fe\text{-}4S]_H$ and $[2Fe]_H$ are shown on top of the data as a solid and dashed line, respectively.

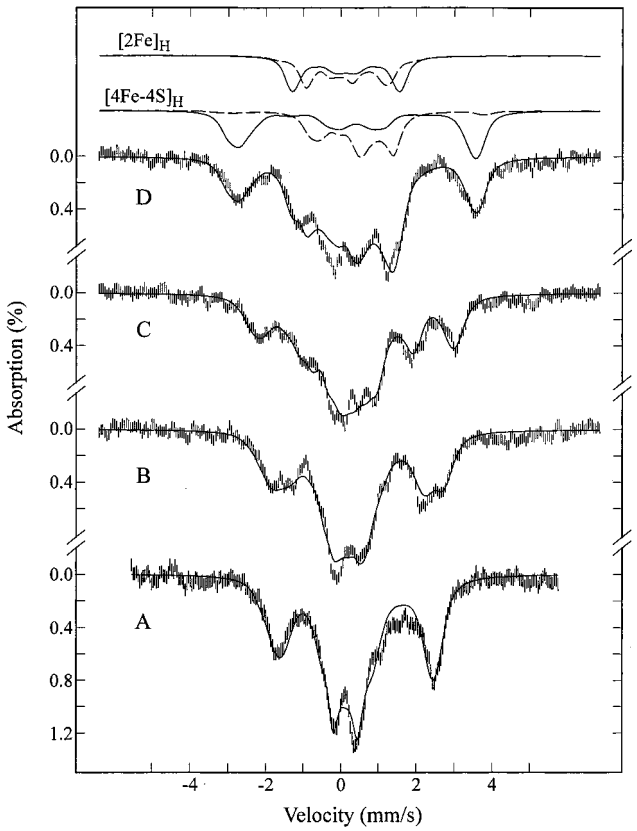

Figure 10. Field-dependent Mössbauer spectra of H_{OX}-CO. The data were recorded at 4.2 K in a parallel applied field of 0.05 T (A), 2 T (B), 4 T (C), or 8 T (D). These spectra were prepared from the spectra of the CO-reacted sample by removing the contributions of the F cluster from the raw data using theoretical spectra simulated with parameters listed in Table 2. The solid lines overlaid with the experimental spectra are theoretical simulations using the parameters of H_{OX}-CO listed in Table 3. For the 8 T spectrum, individual spectral components originating from the Fe sites of the $[2Fe]_H$ subcluster (Fe1: dashed line, Fe2: solid line) and $[4Fe\text{-}4S]_H^{2+}$ cluster (pair 1: dashed line, pair 2: solid line) are also shown above spectrum E.

data have provided direct evidence supporting our previous suggestion that the conversion of $H_{OX-2.06}$ to $H_{OX-2.10}$ does not represent a reduction on the H cluster, and hence, the conversion is likely to reflect a conformational change. The Mössbauer results have further revealed that, in $H_{OX-2.06}$, the reducing equivalent is located on the $[4Fe\text{-}4S]_H$ subcluster, while in $H_{OX-2.10}$ it is localized on the $[2Fe]_H$ subcluster. Consequently, this irreversible conformational change must alter the redox properties of either one or both subclusters of H to promote the transfer of an electron from the $[4Fe\text{-}4S]_H$ subcluster to the $[2Fe]_H$ subcluster. Specific details of the conformation change that causes the redistribution of the reducing equivalent are currently not known.

Oxidation States of the $[2Fe]_H$ Subcluster. For high-spin Fe ions, the Mössbauer isomer shift, δ, is a useful parameter for determining Fe oxidation states, because the δ values for high-spin ferrous and ferric states are significantly different. Depending on the coordination environment, high-spin ferrous ions generally exhibit δ values that are 0.4−0.7 mm/s larger than that of the ferric ions, with the lower end corresponding to tetrahedral sulfur coordinations[31,32] and the higher end corresponding to hexacoordinate N/O coordinations.[33] For low-spin Fe ions, the oxidation-state dependence of δ is less clear, particularly in the cases involving strong ligands such as CN and CO. For example, the isomer shifts of Fe cyanide complexes have been shown to be insensitive to the oxidation states of the Fe.[34] In biology, low-spin Fe states are mostly found in heme proteins. In general, the δ values (∼0.45 mm/s) of low-spin ferrous heme are about 0.15 mm/s larger than the corresponding ferric δ (∼0.3 mm/s). However, binding of CO reduces the ferrous δ value to be practically indistinguishable from the ferric value.[35] Consequently, the presence of the strong CO and CN ligands in the binuclear $[2Fe]_H$ subcluster not only ensures that the Fe atoms are in the low-spin states but also makes it difficult to assign Fe oxidation state by using the isomer shift parameter.

Since the publications of the crystal structures of the NiFe[36] and Fe hydrogenases,[11,13] several Fe model complexes with mixed S/CN/CO ligand coordination have been synthesized and characterized.[24,37−39] A few of these complexes have also been

(31) Schulz, C.; Debrunner, P. G. *J. Phys. (Paris), Colloq.* **1976**, 153−158.

(32) Moura, I.; Huynh, B. H.; Hausinger, R. P.; Le Gall, J.; Xavier, A. V.; Münck, E. *J. Biol. Chem.* **1980**, *255*, 2493−2498.

(33) Greenwood, N. N.; Gibb, T. C. *Mössbauer Spectroscopy*; Chapman and Hall Ltd: London, 1971; pp 112−168.

(34) Greenwood, N. N.; Gibb, T. C. *Mössbauer Spectroscopy*; Chapman and Hall Ltd: London, 1971; pp 169−193.

(35) Debrunner, P. G. *Phys. Bioinorg. Chem. Ser.; Iron Porphyrins, Pt. 3* **1989**, *4*, 137−234.

(36) Volbeda, A.; Charon, M.-H.; Piras, C.; Hatchikian, E. C.; Frey, M.; Fontecilla-Camps, J. C. *Nature (London)* **1995**, *373*, 580−587.

(37) LeCloirec, A.; Best, S. P.; Borg, S.; Davies, S. C.; Evans, D. L.; Pickett, C. J. *Chem. Commun* **1999**, 2285−2286.

(38) Lyon, E. J.; Georgakaki, I. P.; Reibenspies, J. H.; Darensbourg, M. Y. *Angew. Chem., Int. Ed.* **1999**, *38*, 3178−3180.

characterized by Mössbauer spectroscopy.[24,37] Comparing these complexes, the isomer shift values (0.13−0.17 mm/s) determined for the Fe sites of the $[2Fe]_H$ cluster in the *D. vulgaris* hydrogenase are consistent with the value 0.15 mm/s reported for a mononuclear low-spin Fe(II) complex[24] and are considerably larger than those (0.05 and 0.03 mm/s) reported for two low-spin di-Fe(I) complexes.[37] (The values for the di-Fe(I) compounds are recorded at 77 K. To compare with the 4.2 K value, ∼0.02 mm/s should be added to the 77 K values.) On the basis of this observation, we are currently in favor of an Fe(II)/Fe(III) assignment for the Fe sites in the $[2Fe]_H$ subcluster (see below). With the limited data available, an alternative Fe(II)/Fe(I) assignment, however, is equally probable.

According to the Mössbauer results, one Fe site of the $[2Fe]_H$ subcluster in $H_{OX-2.10}$ as well as in H_{OX}-CO exhibits magnetic hyperfine interaction while the other site is diamagnetic. With the premise of Fe(II) and Fe(III) being the potential oxidation states for the Fe sites in $[2Fe]_H$, the diamagnetic site can only be assigned to a low-spin Fe(II), thus leaving the paramagnetic site to be assigned to a low-spin Fe(III). The parameters ΔE_Q and δ determined for these two sites (in both $H_{OX-2.10}$ and H_{OX}-CO) are very similar, supporting the argument that the δ values are insensitive to the oxidation states of low-spin Fe(II)/Fe(III) complexes with CN and CO ligands. The assignment of a mixed-valent low-spin Fe(II)Fe(III) state for the binuclear $[2Fe]_H$ cluster is consistent with the $S = {}^1/_2$ ground state determined by the EPR measurements. The assignment of a low-spin Fe(III) to the paramagnetic site, however, is inconsistent with the observed isotropic *A* values, since low-spin Fe(III) generally exhibits anisotropic magnetic hyperfine interactions due to the large unquenched orbital angular momentum.[40] This lack of anisotropy in the magnetic hyperfine interaction for the paramagnetic site of the $[2Fe]_H$ subcluster has also been observed for the CO-inhibited *C. pasteurianum* hydrogenase II.[22] The inconsistency between the observed isotropic *A* value and the low-spin Fe(III) assignment was first noted in the study of the *C. pasteurianum* enzyme and has been thoroughly discussed.[22] Currently, there exists no satisfactory explanation for this inconsistency.

As mentioned above, due to the limited reference data available and the lack of sensitivity of the parameter δ toward the oxidation state of low-spin Fe complex with strong ligands, an Fe(II)Fe(I) assignment for the $[2Fe]_H$ cluster in $H_{OX-2.10}$ and H_{OX}-CO is equally probable. In this scenario, the paramagnetic site would have to be assigned to a low-spin Fe(I). For low-spin Fe(I), the unpaired electron is expected to reside on an e_g orbital, which would also produce substantial anisotropy in *A*. Consequently, the lack of anisotropy in *A* observed for the paramagnetic site would also be difficult to explain with this alternative assignment.

In H_{OX+1} and H_{red}, the $[2Fe]_H$ subcluster is diamagnetic, and the two Fe sites are spectroscopically indistinguishable. These observed properties are consistent with the binuclear center consisting of either two ferrous low-spin ions or two antiferromagnetically coupled low-spin ferric ions. The insensitivity of the parameters toward Fe oxidation state does not allow us to distinguish between these two alternatives. Since the enzyme is purified aerobically, it may be reasonable to assume that the $[2Fe]_H$ cluster in H_{OX+1} is in a diferric state. A diferric assignment for $[2Fe]_H$ in H_{OX+1} would be consistent with the Fe(II)Fe(III) assignment for $H_{OX-2.10}$, which is presumably further reduced than H_{OX+1}. Alternatively, a diferrous assignment for $[2Fe]_H$ in H_{OX+1} would yield an Fe(II)Fe(I) assignment for $H_{OX-2.10}$. For H_{red}, the situation is unclear. Although a diferrous state is an obvious possibility since the sample is prepared at −350 mV, consideration of the enzyme function suggests that a diferric state is also probable. *D. vulgaris* hydrogenase is an efficient bi-directional hydrogenase. At −350 mV and under an Ar atmosphere, protons are reduced and hydrogen is evolved. If electron transfer from the F clusters to the H cluster is the rate-limiting step, fast reduction of protons would have retained the H cluster in the oxidized form. However, it is important to point out that this oxidized form of the H cluster may be structurally different from that of H_{OX+1} since the cluster has undergone reductive activation.

Binding of Exogenous CO with H Cluster in *D. vulgaris* Hydrogenase. In this manuscript, we have used Mössbauer spectroscopy to investigate the CO-reacted *D. vulgaris* hydrogenase. Detailed analysis of the data has yielded characteristic parameters for the CO-bound H cluster, H_{OX}-CO. The results indicate that H_{OX}-CO is isoelectronic with $H_{OX-2.10}$. This conclusion is supported by previous EPR investigations which showed that H_{OX}-CO is photosensitive and can be reversibly converted into $H_{OX-2.10}$ by illumination at temperatures below 10 K.[17] Further, the results presented here indicate not only that H_{OX}-CO is isoelectronic with $H_{OX-2.10}$, but also that its electronic distribution is very similar to that of $H_{OX-2.10}$. Both H_{OX}-CO and $H_{OX-2.10}$ can be described as a cuboidal $[4Fe\text{-}4S]_H^{2+}$ cluster exchange coupled to a $S = {}^1/_2$ mixed-valent $[2Fe]_H$ subcluster via a corner Fe of the cube. The major difference between these two states is that H_{OX}-CO has a significantly larger j/Δ ratio, where j is the strength of the exchange coupling and Δ is the energy separation between the singlet ground state and the triplet excited state of the $[4Fe\text{-}4S]_H^{2+}$ cube. Since the ΔE_Q and δ parameters determined for the $[4Fe\text{-}4S]_H^{2+}$ subcluster are very similar for H_{OX}-CO and $H_{OX-2.10}$, the electronic structure and, thus, the energy separation Δ are not expected to be significantly different for H_{OX}-CO and $H_{OX-2.10}$. The observed increase in j/Δ for H_{OX}-CO, therefore, must represent an increase in the exchange coupling constant j, which may arise either from a conformational change involving the covalent bonds between the two exchange-coupled subclusters or by changing the electronic distributions of $[2Fe]_H$. The former is considered to be unlikely on the basis of the following two lines of arguments. First, EPR investigation has shown that H_{OX}-CO is photosensitive and can be converted into $H_{OX-2.10}$ by illumination at temperatures below 10 K.[17] Since the conversion happens at such a low temperature, structural changes are unlikely. Second, X-ray crystallographic investigations on *C. pasteurianum* hydrogenase I revealed that an exogenous CO binds to Fe2[19] and that this binding can be cleaved photolytically.[20] Photolysis of the CO was found to shorten the Fe2-bridging carbonyl bound from 2.09 Å in the CO-bound form to 1.85 Å in the photolyzed form,[20] but no significant changes on the iron-bridging cysteine-iron bonds linking the two subclusters were reported. Further, EPR measurements on the *C. pasteurianum* hydrogenase I crystals indicate that the CO-bound form of the H cluster in the crystals is indeed corresponding to the $H_{OX\text{-}2.06}$ state.[41] Since the structure of the H cluster for the *D. vulgaris* hydrogenase is practically identical to that of the *C. pasteurianum* hydrogenase I, similar exogenous CO binding mode and photolysis effects are expected for both enzymes. In other words, significant changes involving the bonds connecting the subclusters upon CO binding are unlikely. Consequently, the increase in j may

(39) Schmidt, M.; Contakes, S. M.; Rauchfuss, T. B. *J. Am. Chem. Soc.* **1999**, *121*, 9736−9737.

(40) Oosterhuis, W. T.; Lang, G. *Phys. Rev.* **1969**, *178*, 439−456.

(41) Bennett, B.; Lemon, B. J.; Peters, J. W. *Biochemistry* **2000**, *39*, 7455−7460.

reflect a change in the electronic distribution of the $[2Fe]_H$ subcluster. The following proposed scenario might explain the observed increase in *j* upon CO binding. In the unligated $H_{OX-2.10}$ state, Fe1 is the diamagnetic Fe(II) site and Fe2 the paramagnetic $S = {}^1/_2$ Fe(III) or Fe(I) site. With the paramagnetic site located at a four-bond distance away from the [4Fe-4S] cube, the coupling is expected to be weak. Binding of CO at Fe2 causes a redistribution of the unpaired electron between the two iron sites, resulting in Fe1 being the paramagnetic site and Fe2 the diamagnetic site. The observed increase in *j* could then be explained as a consequence of reducing the bonding distance between the [4Fe-4S] cube and the $S = {}^1/_2$ center by shifting the paramagnetic site from a four-bond distant Fe2 to Fe1, which is covalently linked to the [4Fe-4S] cube via a single cysteine sulfur. Obviously, further investigations are required to assess the validity of this proposal.

Acknowledgment. We thank Drs. Jean LeGall, Daulat S. Patil, and Shao H. He for the growth of *D. vulgaris* and for purification and characterization of the hydrogenase. This work is supported in part by grants from the National Institutes of Health (GM 47295 and GM 58778 to B.H.H.) and from PRAXIS (to J.J.G.M. and I.M.).

JA003176+